ISSN 0554-6397
Prethodno priopćenje
(*Preliminary communication*)

Ivan Sulovsky
E-mail: ivan.sulovsky@uniri.hr
Jasna Prpić-Oršić
E-mail: jasna.prpic.orsic@uniri.hr
University of Rijeka, Faculty of Engineering, Vukovarska 58, 51000 Rijeka, Croatia

On the Development of Numerical Ocean for Seakeeping Simulations in Openfoam®

Abstract

The ongoing trend of using numerical simulations in marine hydrodynamics yields the need to describe the potential of developing a numerical environment relevant for seakeeping simulations in CFD, more precisely in an open-source software OpenFOAM®. In that manner, the main objective of this paper is to investigate the numerical parameters that affect the well-known issues of dissipative and dispersive errors that are present with long gravity-driven waves within the finite volume method. Grid refinement studies are conducted to find a compromise between accuracy and computational cost. The performance of various methods for the discretization of the temporal derivatives in Navier-Stokes equations is investigated along with the convective term discretization. Gradient schemes are also investigated since their choice can heavily influence the pressure calculation and consequently, the forces acting on the floating body. Furthermore, the inclusion of a standard two-equation turbulence modelleads to an undesirable build-up of turbulent viscosity bellow the free surface, resulting in wave damping. Therefore, turbulence modelling is also addressed with standard turbulence models together with stabilized versions, specific for wave applications. Finally, a combination of optimal settings is proposed and tested. Potential applications of the numerical ocean are discussed, especially with respect tothe problem involving seakeeping and propulsion in irregular waves.

Keywords: Numerical ocean, OpenFOAM®, free surface flows, irregular seas

1. Introduction

In the last two decades, numerical simulations have steadily made their way to the forefront in the toolset of the designer of ships and offshore structures. The complexity of the engineering challenges together with increasing computational power has yielded significant advances in the field of computational continuum mechanics. Therefore, assessing the reliability and accuracy of numerical methods should be an obligatory a priori engineering procedure. In the context of computational marine hydrodynamics,

wave modelling has advanced in recent years, specifically toward reducing the needed computational resources. Also, the wanted level of physical accuracy prescribes the necessary hydrodynamic model. For seakeeping problems, potential flow codes have proven their reliability however, advanced simulations including propulsion modelling or maneuvering, cannot properly capture the flow phenomenons if the simulation accounts for inviscid, irrotational and if the focus is on slamming events and incompressible fluid.

In surface wave modelling, two main sources of errors are present within the finite volume method: dissipative errors, if the grid resolution is insufficient in the free surface area which leads to a lower wave amplitude than desired. Also, dispersion errors are due to unwanted wave reflections from the outlet boundary in the case of head waves, and on side boundaries in the case of oblique waves. It is a common practice in computational marine hydrodynamics, to assess the aforementioned errors in the numerical model if waves are included in the simulation. Yan et al [1] investigated the influence of time-step and mesh resolution on wave amplitude and length. Also, convergence studies for the different numerical wave-making methods in OpenFOAM® were done by Windt et al. [2]. These procedures are practically omitted if one is using commercial CFD codes; mesh refinement and time-step are automatically set to reduce the errors within an acceptable range. In this paper, we examine the influence of several numerical parameters in the Reynolds-Average Navier-Stokes equations (RANSE) that affect the numerical solution of irregular long-crested seas delivered by the finite volume method. More precisely, research is conducted on the effects of the discretization schemes for temporal derivatives, gradient terms, and divergence of velocity, and finally, the influence of turbulence modelling is addressed.

Regarding the temporal derivatives, three schemes are investigated. Backward and Crank-Nicolson schemes as the 2^{nd} order ones, and Euler 1^{st} order scheme. The choice of these schemes represents leverage between accuracy and stability since 2^{nd} order schemes introduce less numerical diffusion into the accuracy, however, with a higher possibility of simulation diverging. Furthermore, two gradient discretization schemes are investigated, namely the scheme based on the Gauss theorem with linear interpolation and the scheme based on estimating gradient value using the least squares method. The next step is to investigate three schemes for the calculation of divergence for velocity. Gauss linear upwind and Van Leer schemes are employed as 2^{nd} order ones, and QUICK scheme as a high-order scheme. Lastly, two turbulence models are investigated. The *k*-ωSST model [3] and realizable k-ε model. All calculations in this study are conducted employing an open-source CFD toolbox OpenFOAM® [4]. Simulations are based on a two-dimensional space to reduce the computational time. This paper is organized as follows: in the second chapter, the standard numerical model from OpenFOAM® is briefly described. An overview of the numerical parameter along with the computational mesh and boundaries are depicted. In Chapter 3., the proposed design of numerical experiments is explained which is followed by a clarification of the parameters by which the performance of certain schemes are evaluated. This is followed

by a chapter with results where subchapters are divided according to the schemes that are being researched. Lastly, the results are briefly discussed in the last chapter.

2. Numerical model

Numerical details of the method used in this study are outlined. For simulations of fluid flow, the finite volume method of discretization has become dominant. OpenFOAM® is based on a cell-centered finite volume method in which the fluid flow is driven by the Navier-Stokes equations of mass conservation (1) and momentum conservation (2). The incompressibility of the fluid is assumed.

$$\nabla \cdot \boldsymbol{u} = 0 \tag{1}$$

$$\frac{\partial \boldsymbol{u}}{\partial t} + \boldsymbol{u} \cdot (\nabla \cdot \boldsymbol{u}) - \nu \nabla^2 \boldsymbol{u} = g - \nabla p \frac{1}{\rho}) \tag{2}$$

Terms in equations (1) and (2) are as follows: **u** stands for fluid velocity, is the effective kinematic viscosity, ∇p is the pressure gradient. Gravitational acceleration is denoted as g and fluid density as ρ. The interface between air and water in the free surface zone is modelled using a geometric *Volume of Fluid* (VOF) technique, developed by Roenby [5]. In the VOF method, indicator function α is introduced in the equations. It models the effective kinematic viscosity ν and density ρ for different fluids, in this case, air and water, as depicted in equations (3) and (4).

$$\rho = (1-\alpha)\rho_{air} + \alpha\rho_{water} \tag{3}$$

$$\nu = (1-\alpha)\nu_{air} + \alpha\nu_{water} \tag{4}$$

Boundary conditions are specified for each set of faces (patches) at the edge of the domain. A schematic overview of the boundary faces is depicted in Fig.1. Computational grid is created using *snappyHexMesh,* an embedded meshing tool within OpenFOAM®. To significantly decrease the computational cost, a 2D solution is sought. It is presumed that the various nonlinear, three-dimensional effects present in free surface waves are of interest only for rough sea states and with the occurrence of wave breaking. Thus, the total number of cells is approximately $15 \cdot 10^3$ with a maximum non-orthogonality of 18.43. The coupling of pressure-velocity is initialized with a PIMPLE algorithm with two iterations for pressure residuals and two for a momentum matrix. Regarding linear solvers, pressure is solved using a PCG solver while the velocity and turbulence terms are with Gauss-Seidel. To ensure the numerical stability of the simulations, the Courant number at the free surface is kept under 0.2 while the global Courant number is

kept below 2. Consequently, the time-step is set to 5^{-3} seconds. Discretization schemes are not discussed here since their effects are investigated further in the text. Simplified 2D topology of the domain is depicted in figure 1. while the refinements of the mesh can be seen in figure 2.

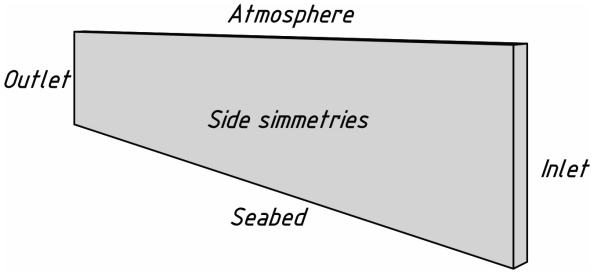

Figure 1: Topology of the computational domain

On the inlet faces, oscillatory boundary conditions of velocity and α are imposed for wave build-up. Sidewalls of the domain are given a symmetrical boundary condition. Ground and atmosphere patches are given a standard boundary condition according to ITTC standards [6]. The length of the domain is set to 1400 meters. Configuration of the deep-sea environment is adopted with a sea depth of 720 m.

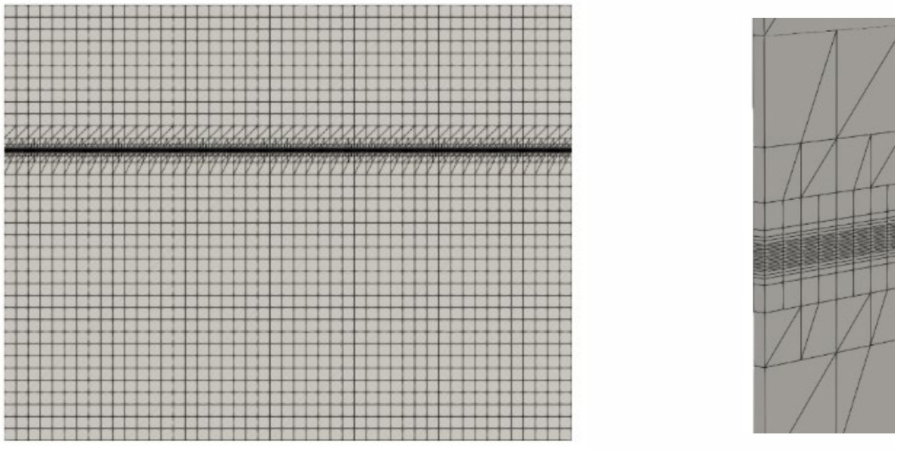

Figure 2: a) Computational domain *b) Free surface refinement*

For the prevention of unwanted wave reflections, a relaxation zone is set on the control volumes towards the outlet boundary [7]. Grid refinement study is omitted in this work since it has been thoroughly researched. Also, it is difficult for irregular waves to decipher the optimum grid size since the wave amplitudes and periods are inherently different in time.

3. Design of experiments

In this section, the design of simulation experiments is described along with the selected wave spectrum. The purpouse of conducting design of experiments is the wanted quality of the end product itself. In this context, this experiments will show the optimal choice of numerical schemes for more complex, three-dimensional simulations that ehxibit high computaional resources. The experimental design is constructed within four layers. Firstly, the influence of numerical schemes for solving temporal derivatives and their level of order is investigated. Backward and Crank-Nicolson schemes are chosen as the second-order ones while the Euler scheme is first-order accurate. Secondly, the focus is set on the discretization of gradient terms. Gauss theorem with linear interpolation is investigated along with the least squares method. After gradient discretization, different divergence schemes for velocity are researched. Lastly, the influence of different turbulence models relevant to marine hydrodynamics is evaluated. The distribution of wave amplitudes is set according ITTC wave spectrum [8] with a significant wave height $H_{1/3}$ of 2.38 meters and peak period of 7.77 s, depicted in equation (5).

$$S(\omega) = \frac{A}{\omega^5} e^{\frac{-B}{\omega^4}} \tag{5}$$

With coefficients A and B described in equations (6) and (7).

$$A = 173 \frac{H_{1/3}^2}{\bar{T}^4} \tag{6}$$

$$B = -\frac{692}{\bar{T}^4} \tag{7}$$

$H_{1/3}$ is the significant wave height and T is the mean peak wave period. Mean flow speed is set to 5.27 m/s which corresponds to the ship speed which can be entirely arbitrary. Since the implementation of irregular seas in OpenFOAM® requires distinct values for each wave amplitude, phase, and period, theoretical wave amplitudes are derived from the frequency spectrum through equation (8):

$$\zeta_i = \sqrt{2S(\omega)\Delta\omega} \tag{8}$$

Where is the difference in wave frequency between the previous wave amplitude and the current one. Since irregular waves consist of randomly scattered wave characteristics, the range of wave periods is taken according to Tucker [9] with modified lower cut-off frequency :

$$0.5T < T_P < 1.85T$$

The distribution of wave phase ϕ is set as a random following equation (9):

$$\phi = 2\pi \cdot r \tag{9}$$

Where r can take an arbitrary value between zero and one. Finally, synthetic wave series of 100 wave components are generated as reads in equation (10):

$$\zeta = \sum_{i}^{N} (\zeta_i \cdot \cos(\omega t + \phi)) \tag{10}$$

For quantifying the difference between the numerical solution and a target value, significant wave height is retrieved from the time signal, equation (11):

$$H_{1/3-CFD} = 4 \cdot \sigma \tag{11}$$

Where is the standard deviation of the signal. The ITTC wave spectrum shape is represented in Figure 3.

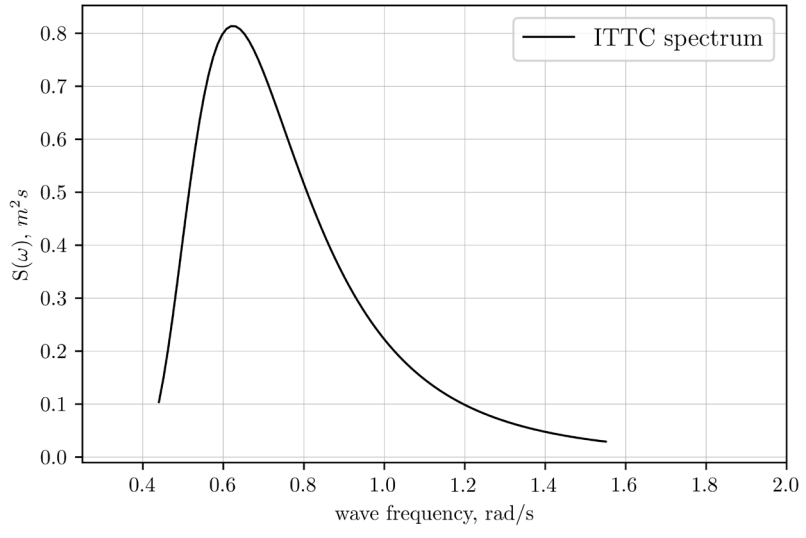

Figure 3: ITTC wave spectrum

The section concludes with a schematic overview of the proposed experimental design, Figure 4. The initial characteristics of each layer in the design of experiments is the backward scheme for temp. derivatives, Gauss linear scheme for gradient discretization and Gauss linear upwind scheme for the divergence of velocity. Turbulence terms are omitted until the last layer of inspecting the turbulence models.

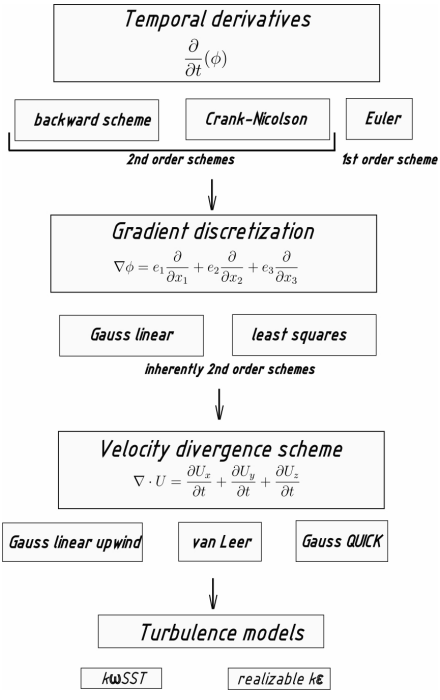

Figure 4: Schematical overview of the experimental design

4. Results

The results of the numerical simulations are presented in this section. All computations are done on a desktop workstation, distributing the workload to eight processors. The presentation of the results is divided into subsections for more clear representation. Before jumping into the results, a brief description of post-processing is given. Every subsection consists of a table in which the calculated value of significant wave height $H_{1/3\text{-}CFD}$ is compared with the target value of $H_{1/3\text{-}CFD}$. Difference from target value is given in percentage in which index $^-$ indicates underprediction while $^+$ overprediction. After the tables, plots of the power spectral densities are presented where on the horizontal axis are wave periods. In that manner, wave frequencies e.g., obtained wave periods are compared, as it is difficult to assess in the time domain.

4.1. Investigation of temporal derivatives

The level of order of the numerical schemes for temporal derivatives can have a strong influence on wave propagation. 1st order schemes are known for excessive numerical diffusion while 2nd order schemes can introduce instability in the simulation despite the increased accuracy. In Table 1. the results of the significant wave height from CFD are compared with a target value.

Table 1: Results for different time schemes

	$H_{1/3\text{-}CFD,\ m}$	Difference from the target value, %
Backward 2nd order	2.213	7-
CN 2nd order	2.12	7-
Euler 1st order	2.567	7.8+

Power spectral density plots for different time schemes are given in Figure 5.

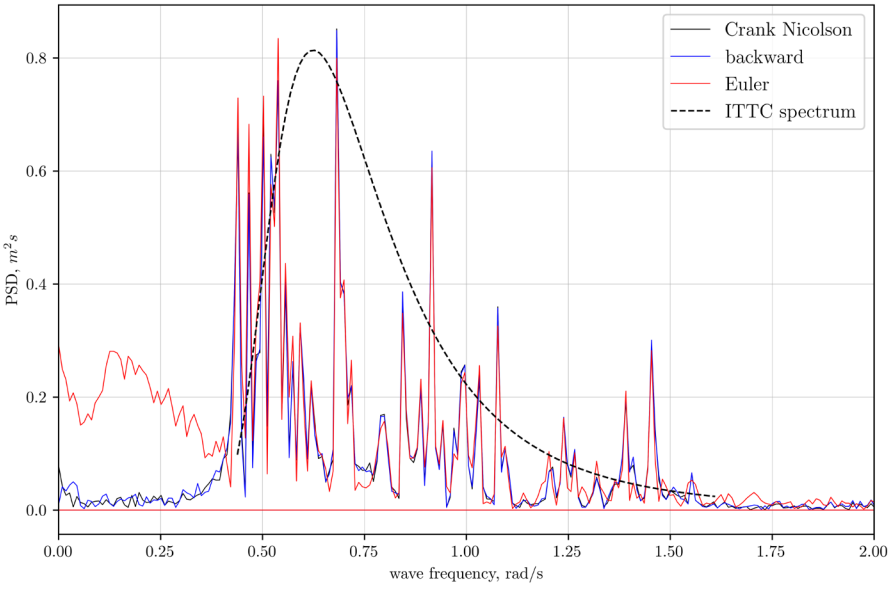

Figure 5: PSD for different time schemes

4.2. Investigation on gradient discretization

Two gradient schemes are investigated. Gauss linear scheme, based on the

Gaussian integration which is a standard approach in finite volume discretization. Also, a scheme based on the least squares method is investigated [11]. The selection of these schemes should be influenced by the mesh quality e.g., if the mesh non-orthogonality is high, a scheme based on the least squares method should improve the stability of the simulation. In Table 2. the results of the significant wave height from CFD are compared with a target value.

Table 2: Results for different gradient discretization schemes

	$H_{1/3\text{-}CFD,\ m}$	Difference from tar. value, %
Gauss linear 2nd order	2.213	7-
Least squares2nd order	2.203	7.5-

Power spectral density plots for different time schemes are given in Figure 6.

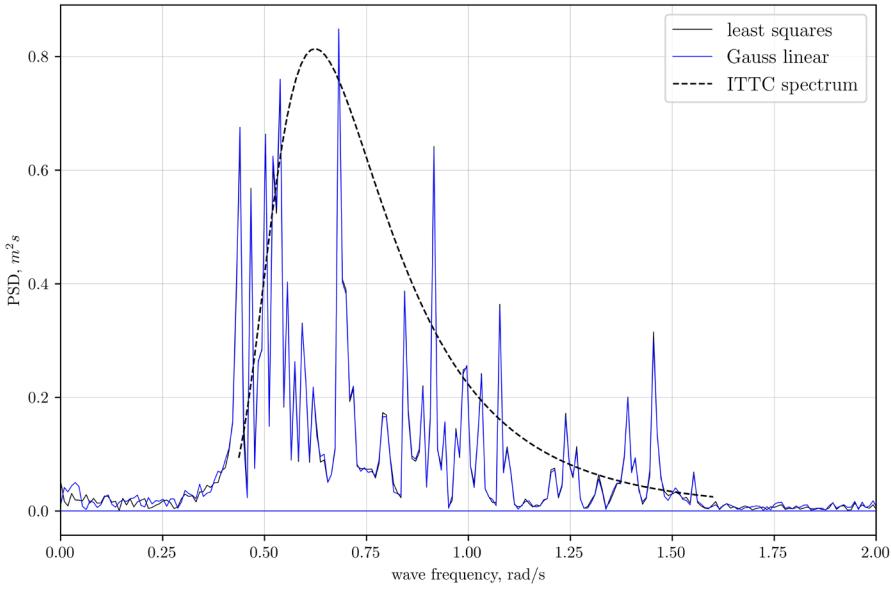

Figure 6: PSD for different gradient schemes

4.3. Investigation of velocity divergence schemes

Three divergent schemes are investigated. Gauss linear and van Leer [10] schemes are both in the family of the 2nd order, unbounded schemes. The last scheme investigated is the QUICK (Quadratic Upstream Interpolation for Convective kinematics) scheme

[12] which avoids the stability problems of central differencing but also avoids artificial numerical diffusion that is associated with upstream differencing. For the convection term, QUICK is 3rd order accurate in space and 1st order accurate in time. In Table 3. the results of the significant wave height from CFD are compared with a target value.

Table 3: Results for different velocity divergence schemes

	$H_{1/3\text{-}CFD,\ m}$	Difference from tar. value, %
Gauss linear	2.213	7-
Gauss QUICK	2.285	3.95-
Van Leer	2.203	8.4-

Power spectral density plots for different time schemes are given in Figure 5.

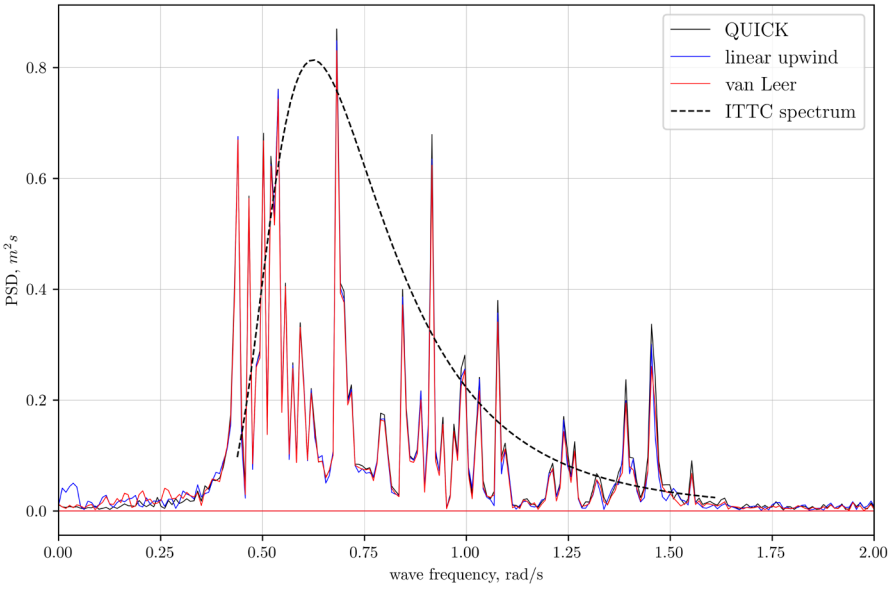

Figure 7: PSD for different velocity divergence schemes

4.4. Investigation of turbulence models

As the last part of the design of experiments, the effects of two different turbulence models most commonly used in marine hydrodynamics are investigated. The first model is the realizable kε model, which offers some improvements concerning the standard kε model. Improvements involve better performance for flows with rotation

and boundary layer separation under strong adverse pressure gradients. The second model is the kωSST (Shear Stress Tensor) model which is a blend between the standard kω and kε model. Turbulence models can have a strong influence over the wave height since their formulation can induce artificial turbulent viscosity building beneath the wave which dampens the wave itself. Stabilized versions of turbulence models are offered by Larsen and Fuhrman [13] but are not investigated in this paper. In Table 4. the results of the significant wave height from CFD are compared with a target value.

Table 4: Results for different turbulence models

	$H_{1/3\text{-}CFD,\ m}$	Difference from tar. value, %
realizable kε	2.213	7-
kωSST	2.285	3.95-

Power spectral density plots for different time schemes are given in Figure 8.

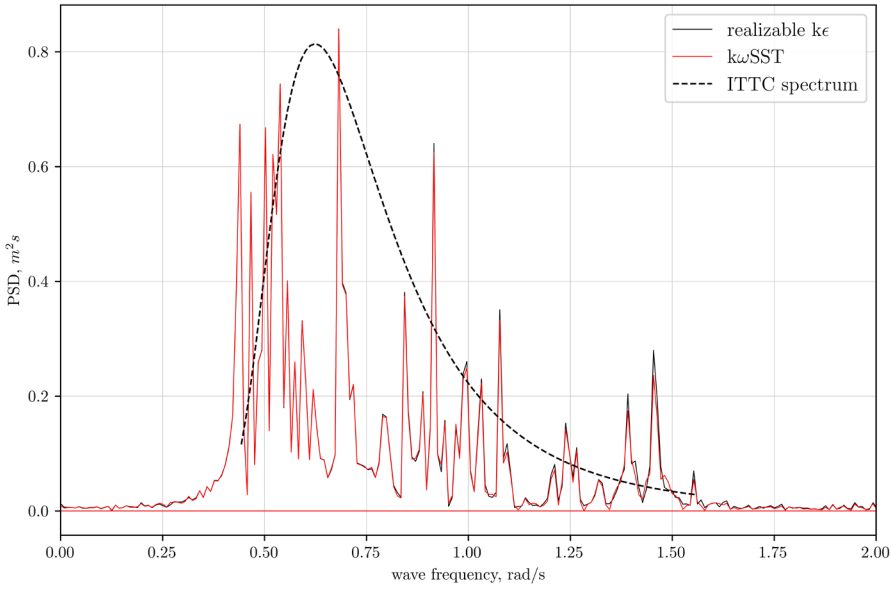

Figure 8: PSD for different turbulence models

5. Discussion of the results

No significant influence of selected numerical schemes is noticed on the observed significant wave height. The QUICK scheme makes an exception, as seen in chapter 4.4. For the aforementioned scheme, the discrepancy between the numerical wave height and the targeted is the smallest. As seen in Figure 1., waves with increased wavelength are present for the Euler 1st order scheme however, their magnitude and frequency are outside of the targeting wave spectrum. Gradient discretization schemes yield practically the same result despite their fundamentally different approach to gradient estimation. Results for different turbulence models show that only a negligible difference is seen for the frequencies above 1 rad/s.

6. Conclusions

The main objective of this paper is to investigate the effects of different discretization schemes and turbulence models in the simulation of irregular long-crested seas. The design of the experiments starts with the investigation of different numerical schemes for temporal derivatives of the different level of order. Gradient discretization and velocity divergence schemes are investigated, followed by the assessing the effects of different turbulence models on the solution. The performance of each scheme and turbulence model is quantified by a single value of significant wave height, measured numerically at a certain point in the domain. The numerical results are compared with the targeted value of the significant wave height. The final results indicate that there is almost negligible influence of the choice of schemes on the solution. This leads to the conclusion that spatial discretization, e.g. the mesh topology, should be adequately considered despite the choice of numerical schemes. The extention of the model to the fully three-dimensional space are the further steps in this work.

Acknowledgments

This work has been supported by the Croatian Science Foundation under the project IP-2022-10-2821.

References

1. Yan, M.; Ma, X.; Bai, W.; Lin, Z.; Li, Y. Numerical Simulation of Wave Interaction with Payloads of Different Postures Using OpenFOAM. *J. Mar. Sci. Eng.* **2020**, *8*, 433. https://doi.org/10.3390/jmse8060433
2. Windt, C.; Davidson, J.; Schmitt, P.; Ringwood, J.V. On the Assessment of Numerical Wave Makers in CFD Simulations. *J. Mar. Sci. Eng.* **2019**, *7*, 47. https://doi.org/10.3390/jmse7020047
3. Menter, F. R. (1993), "Zonal Two Equation k-ω Turbulence Models for Aerodynamic Flows", AIAA Paper 93-2906.
4. Weller H.G., Tabor G., Jasak H., Fureby C.: *„A tensorial approach to computational continuum mechanics using object-oriented techniques."*, Computers in Physics and IEEE Computational Science&Engineering, November 1998, 12 (6): 620-631 https://doi.org/10.1063/1.168744
5. Roenby, J.; Bredmose, H.; Jasak, H. A computational method for sharp interface advection. *R. Soc. Open Sci.* **2016**, *3*, 160405.
6. ITTC—Recommended Procedures and Guidelines (Practical Guidelines for Ship CFD Applications). Available online: https://ittc.info/media/1357/75-03-02-03.pdf (accessed on 24 November 2023).
7. Jacobsen, N.G.; Fuhrman, D.R.; Fredsøe, J. A wave generation toolbox for the open-source CFD library: OpenFoam®: Wave Generation Toolbox. *Int. J. Numer. Methods Fluids* **2012**, *70*, 1073–1088
8. Bretschneider, C.L., 1959, "Wave variability and wave spectra for win-generated gravity waves", Technical Memorandum No. 118, Beach Erosion Board, U.S. Army Corps of Engineers, Washington, DC, USA.
9. Tucker M.J., Pitt E.G., Waves in Ocean Engineering (1990) ISBN: 9780080435664
10. B. van Leer. Towards the Ultimate Conservative Difference Scheme. II. Monotonicity and Conservation Combined in a Second-order Scheme. *Journal of computational physics*, 14(4):361–370, 1974.
11. S. Muzaferija, D. A. Gosman, Finite-volume CFD procedure and adaptive error control strategy for grids of arbitrary topology, J. Comput. Phys. 138 (1997) 766–787
12. B.P. Leonard. A stable and accurate convective modelling procedure based on quadratic upstream interpolation. *Computer methods in applied mechanics and engineering*, 19(1):59–98, 1979.
13. Larsen B:E.; Fuhrman D.R., (2020) Tutorial for "multiPhaseStabilizedTurbulence in OpenFOAM® - v1912 DOI: https://doi.org/10.11583/DTU.12154713